CARDIFF UNIVERSITY
PRIFYSGOL CAERDYDD

ORCA – Online Research @ Cardiff

This is an Open Access document downloaded from ORCA, Cardiff University's institutional repository:https://orca.cardiff.ac.uk/id/eprint/176582/

This is the author's version of a work that was submitted to / accepted for publication.

Citation for final published version:

Barker, Stephen , Lisiecki, Lorraine E., Knorr, Gregor, Nuber, Sophie and Tzedakis, Polychronis C. 2025. Distinct roles for precession, obliquity, and eccentricity in Pleistocene 100-kyr glacial cycles. Science 387 (6737) , eadp3491. 10.1126/science.adp3491

Publishers page: http://dx.doi.org/10.1126/science.adp3491

Please note:
Changes made as a result of publishing processes such as copy-editing, formatting and page numbers may not be reflected in this version. For the definitive version of this publication, please refer to the published source. You are advised to consult the publisher's version if you wish to cite this paper.

This version is being made available in accordance with publisher policies. See http://orca.cf.ac.uk/policies.html for usage policies. Copyright and moral rights for publications made available in ORCA are retained by the copyright holders.

Title: Distinct roles for precession, obliquity and eccentricity in Pleistocene 100kyr glacial cycles

Authors: Stephen Barker[1]*, Lorraine E. Lisiecki[2], Gregor Knorr[3], Sophie Nuber[1]†, Polychronis C. Tzedakis[4].

Affiliations:

[1]School of Earth and Environmental Sciences, Cardiff University; Cardiff, UK.

[2]Department of Earth Science, University of California; Santa Barbara, USA.

[3]Alfred Wegener Institute, Helmholtz Centre for Polar and Marine Research; Bremerhaven, Germany.

[4]Environmental Change Research Centre, Department of Geography, University College London; London, UK

*Corresponding author. Email: barkers3@cf.ac.uk

†Present address: Department of Oceanography, University of Washington; Washington, USA.

Abstract: Identifying the specific roles of precession, obliquity and eccentricity in glacial/interglacial transitions is hindered by imprecise age control. We circumvent this problem by focussing on the morphology of deglaciation/inception, which we show depends strongly on the relative phasing of precession versus obliquity. We demonstrate that while both parameters are important, precession has more influence on deglacial onset, while obliquity is more important for attainment of peak interglacial conditions and glacial inception. We find that the set of precession peaks (minima) responsible for terminations since 0.9Ma is a subset of those 'candidate peaks' which begin (precession parameter starts decreasing) while obliquity is increasing. Specifically, termination occurs with the first candidate peak following each eccentricity minimum. Thus the gross morphology of 100kyr glacial cycles appears largely deterministic.

Main Text:

Following demonstration that the succession of Quaternary ice ages is fundamentally controlled by changes in Earth's orbital geometry (*1*) many studies have attempted to identify the precise roles of precession, obliquity and eccentricity in the waxing and waning of continental ice sheets, in particular the process of glacial termination (deglaciation). The main obstacles to such an exercise include the closeness in frequency of precession (~1/21kyr) to the 2nd harmonic of obliquity (~1/20.5kyr) and the dating precision required to demonstrate a clear and reproducible link between either parameter and the end of a glacial period. Consequently, there has been considerable debate as to whether precession (*2-5*), obliquity (*6, 7*) or some combination of the two (*8-11*) provides the dominant driving force for glacial termination and moreover as to why glacial terminations tend to be separated by ~100kyr (one of the main periods of eccentricity), hence the '100kyr problem' (*2, 12, 13*). Here we take an alternative approach, based on the assumption that if precession and obliquity play distinct roles in deglaciation, then variations in their relative phasing will be imprinted on the trajectory of ice volume change across individual terminations.

As with previous studies of this type (e.g. *2, 3, 5, 6, 10, 14*) we utilise the record of benthic foraminiferal $\delta^{18}O$ to infer changes in continental ice volume while acknowledging that the signal is influenced by variations in deep ocean temperature (*15, 16*). Indeed, a lead in the timing of mean ocean warming ahead of ice volume decrease across the most recent deglaciation (Termination 1, T1) (*17*) implies a difference of ~2kyr between the $\delta^{18}O$ signal recorded by benthic foraminifera and the component of $\delta^{18}O$ related specifically to ice volume (*18*). However, as we show below, this offset is relatively small compared to the variations in morphology observed (several kyr). Additionally, it has been suggested that the record of benthic $\delta^{18}O$ can be considered a proxy for Earth's energy imbalance (the gain or loss of energy by the ocean-atmosphere system (*17*)) across intervals of ice sheet growth/decay and concomitant ocean cooling/warming (*18*). It could therefore be argued that the results reported here be interpreted in terms of the relative influences of precession and obliquity on Earth's energy imbalance associated with glacial/interglacial (G-IG) variability (see also Supplementary Material).

2. Quantifying deglacial morphology

We begin by quantifying the trajectory of benthic $\delta^{18}O$ across deglacial transitions and interglacials of the 100kyr world (approximately the last 800kyr; Figs. 1, 2). For this we use 3 independent stacks/records of benthic foraminiferal $\delta^{18}O$ (LR04/LR04_untuned (*14, 19*), HW04 (*20, 21*) and U1476pmag (*11*)) on 4 independent timescales (3 of which are free of orbital assumptions; See Methods (*16*)) to calculate the temporal offsets between 4 key points in the curve of $\delta^{18}O$ across each deglacial/interglacial period: (1) the onset of deglaciation (Onset deglac; when $\delta^{18}O$ begins to decrease following a glacial maximum (*16*)), (2) Max deglac: the point at which $\delta^{18}O$ reaches its maximum rate of decrease during termination, (3) Peak IG: the minimum in $\delta^{18}O$ associated with interglacial conditions and (4) Max inception: the subsequent maximum in the rate of $\delta^{18}O$ increase, marking a return to glacial conditions.

We do not define transitions between glacial and interglacial state based on a threshold in (e.g.) sea level or $\delta^{18}O$ (*10, 22*). Instead the points we select represent dynamical boundaries in the curve of $\delta^{18}O$ (e.g. Peak IG represents the change from decreasing to increasing $\delta^{18}O$ while Max

deglac represents the maximum rate of deglaciation). As previously suggested (*23*) this approach has the advantage of providing logical points in the climate curve that we might expect to align with maxima (or minima) in forcing (e.g. we may expect that the maximum rate of ice loss during deglaciation should correspond to a maximum in the forcing responsible). We nevertheless think it is useful to adhere to common nomenclature (e.g. for describing glacial versus interglacial periods). We therefore follow the traditional marine isotope stratigraphic definition of an interglacial as a broad minimum in $\delta^{18}O$ bounded by sharp transitions to heavier values (*24*), which in this case are delineated by Max deglac and Max inception. By this definition an interglacial is divided into a period of deglaciation and a period of glacial inception (Fig. 2A).

Our analysis suggests that variability in the total duration of deglaciation (from Onset deglac to Peak IG) is dominated by large (several kyr) changes in the offset between Max deglac and Peak IG (i.e. late deglaciation, which is equivalent to the deglacial phase of an interglacial; Figs. 1C; 2A) while the offset between Onset deglac and Max deglac (early deglaciation) is comparatively constant (8.6±1kyr for LR04 or 8.9±0.4kyr if Termination T8 is excluded, 7.8±0.9kyr for HW04 and 10±1.7kyr for U1476pmag; Fig. S2F). The interval between Peak IG and Max inception (the inception phase of an interglacial) is also relatively invariant (as previously observed (*25*)), with the offset between Max deglac and Max inception being strongly correlated to that between Max deglac and Peak IG (R^2 = 0.96/0.99 for LR04/LR04_untuned, R^2 = 0.87 for HW04, R^2 = 0.73 for U1476pmag; Figs. 2B, S4). From these results it can be seen that the entire duration from Onset deglac through to Max inception might be predicted simply from the offset between Max deglac and Peak IG.

3. Orbital phasing determines the duration of deglaciation

Previously (*25*) it was suggested that the phasing between precession and obliquity influences the persistence of interglacial conditions. Our results (Fig. 1) suggest that variations in interglacial duration (from Max deglac to Max inception) are dominated by changes in the deglacial phase (i.e. between Max deglac and Peak IG). We might therefore expect to find a relationship between orbital phasing and the offset from Max deglac to Peak IG. To test for such a relationship we need to quantify the phasing between precession and obliquity at the time of each deglaciation. To this end we identify the nearest precession peak to each deglacial transition (i.e. closest to Max deglac) and calculate the offset between that peak and its closest neighbouring peak in obliquity (Fig. 1D). Note that we use the term ‘peak’ (for both obliquity and precession) to describe conditions that give rise to a maximum in northern hemisphere summer insolation (which corresponds to a maximum in obliquity but a minimum in the precession parameter, when northern summer occurs during perihelion).

As stated, attempts to identify which orbital parameter might be more important for deglaciation have been limited by the requirement for accurate and precise age control of paleoproxy records. Our approach is much less sensitive to this requirement. Because we are looking for the closest precession peak to each deglaciation, the age models we employ are required only to have an accuracy of ~±10kyr (for comparison the stated uncertainties for LR04 and HW04 over the last 1Myr are ±4kyr and ±7kyr respectively). Accordingly the set of precession peaks identified for the last 11 terminations within LR04 is exactly the same for all of the records/timescales analysed here (Fig. S2), giving us confidence in the robustness of our selection criteria.

The analysis reveals a strong correlation between Max deglac minus Peak IG and the phasing of precession versus obliquity (Figs. 2C, 2D, S3) with R^2 ranging from 0.74 to 0.88 for the various records and age models employed. Note that the alternative approach, of identifying the closest obliquity peak to Max deglac and its nearest neighbouring precession peak would give an equivalent result but with a negative slope (*16*) (Fig. S5). The observation of such a strong imprint of the phasing between obliquity and precession on the evolution of $\delta^{18}O$ across deglaciation implies not only that both parameters might play a role, but that these roles are somehow discrete (distinct), and therefore distinguishable.

4. Discrete roles for precession and obliquity in deglaciation and glacial inception

Previous studies have emphasised the importance of decreasing obliquity for glacial inception (*11, 25*). However, recent attempts to provide more precise constraints on the timing of glacial termination have reached different conclusions about the relative importance of obliquity versus precession for the onset of deglaciation (*5, 7*). Our results (Fig. 2) show that the duration from Max deglac through to Max inception is a linear function of the offset between peak precession and peak obliquity at the time of deglaciation. We suggest this implies that one parameter plays a more important role in the earlier stages of deglaciation (up to and including Max deglac) while the other is more influential on the latter stages and ultimately the subsequent glacial inception. To evaluate the alternative possibilities we compare 3 hypothetical scenarios (Figs. 3, 4).

In Scenario I we assume that the published age models for each record are accurate. This allows us to identify any significant relationships implied between each key point and the phase of precession or obliquity. For example, in Figure 3 we show results for two deglaciations (T2 and T5) with contrasting orbital phasing. We note that for T2, Max deglac is aligned (roughly) with maximum obliquity and decreasing precession (meaning that summers are intensifying). For T5, Max deglac is roughly aligned with peak (minimum) precession and rising obliquity. In both cases the subsequent Max inception is aligned with a positive precession parameter and low to minimum obliquity.

In Scenarios II and III we make the assumption that there should be a consistent relationship between Max deglac and the phase of whichever orbital parameter is responsible for the onset of deglaciation. Therefore in Scenario II we force Max deglac to align with the peak in precession closest to each termination and assess the implied alignment of Peak IG and Max inception with respect to the phase of obliquity. In Scenario III we align Max deglac with peak obliquity and assess the implied alignment of Peak IG and Max inception with respect to precession. We expect these implied alignments to be stronger when the correct starting parameter is selected, given the observed correlation between Max deglac - Peak IG versus orbital phasing. Our choice to set Max deglac to align with a peak in either parameter follows the logic that the maximum rate in ice volume decrease should coincide approximately with a maximum in forcing (*23*). On the other hand the exact phase employed is not critical for the arguments that follow, only that the phase is consistent for each termination.

For the example of T2 and T5 (Fig. 3) alignment of Max deglac with peak precession (Scenario II) results in alignment of Max inception with low to minimum obliquity in both cases i.e. Max inception for T2 and T5 are aligned consistently with respect to the phase of obliquity, which would be expected if precession is the correct starting parameter. This is not the case for Scenario III, in which alignment of Max deglac with peak obliquity results in Max inception

being aligned with a maximum or minimum in precession for T2 and T5 respectively (i.e. Max inception for T2 and T5 are not aligned consistently with respect to the phase of precession). From this limited example we would therefore select Scenario II as the most likely.

In Figure 4 we plot full results for each scenario for the 3 untuned age models over the last 1Myr (results including LR04 are given in Table S2). This interval includes 11 glacial terminations, but we exclude T1 because it has no subsequent inception. Results for Scenario I reveal a broad scatter of Max deglac around peaks in both obliquity and precession (Fig. 4A1, B1; S6A3, B3), suggesting (in keeping with previous studies (*5, 7, 8*)) that both parameters probably play some role in deglaciation. On the other hand obliquity alone seems to influence glacial inception, which is associated with decreasing to low obliquity (again consistent with previous work (*11, 25*)).

For scenarios II and III we use two approaches to assess the implied phasing between Peak IG (and Max inception) with respect to precession/obliquity (Methods (*16*)). Firstly we use the measured offsets between Max deglac and Peak IG (and Max inception) implied by the original age models. Secondly we predict those offsets from the relationships shown in Figures 2 (and S3, S4) based on the observed orbital phasing in each case. In Figure 4 we plot results using the second approach (full results are given in Table S2). Offsets between Onset deglac and Max deglac are measured in all cases.

In Scenario II we observe a strong alignment of Onset deglac with respect to precession (mean resultant vector length, $r = 0.87$, see Methods (*16*); Figs. 4A2, S6C2). This is not surprising given that the offset between Onset deglac and Max deglac is relatively constant (e.g. Fig.1C), but it is notable that the average offset (8.5±1.7kyr before the peak in precession) is just less than half a precession cycle, implying that if Max deglac coincides with peak precession then the onset of deglaciation occurs ~2kyr after northern summer insolation begins to intensify (as a function of precession). In this scenario Onset deglac and Max deglac also align with increasing to high values of obliquity (Figs. 4B2, S6D2,3). In fact we observe stronger alignment in these cases than observed in Scenario I ($r = 0.52$ vs 0.46 and $r = 0.54$ vs 0.44 respectively; Table S2). Thus for Scenario II the onset of deglaciation occurs when northern summer insolation is increasing as a function of both precession and obliquity (implying a dual role for obliquity and precession in the process of deglaciation).

The most outstanding result from Scenario II is the very strong alignment of Peak IG with decreasing obliquity (very close to the maximum rate of decrease) and of Max inception with low to minimum obliquity (Figs. 4B2, S6D4,5). In each case we obtain r values in excess of 0.95, much higher than those obtained in Scenario I (although the phase relationships observed are similar; Table S2). In other words, when Max deglac is set to peak precession, Peak IG and Max inception align precisely with respect to obliquity. Note that using the measured (rather than predicted) offsets between Max deglac and Peak IG (and Max inception) also gives r values greater than observed in Scenario I ($r = 0.82$ vs 0.64 and $r = 0.72$ vs 0.57 respectively; Table S2). The relationships between Peak IG and Max inception versus precession in Scenario II are not significant.

In Scenario III (Figs. 4B3, S6F3) we observe a strong alignment of Onset deglac with increasing obliquity (Fig. S6F2), analogous to Onset deglac versus precession in Scenario II. However, the relationships between Peak IG and Max inception versus precession are weak ($r < 0.4$) and although statistically significant for the combined records, this is not the case for any record

when treated individually (Table S2). Notably in Scenario III, the relationships between Onset deglac and Max deglac versus precession are significantly worse than in Scenario I (Figs. 4A3, S6E2,3; Table S2) and imply that deglaciation is essentially independent of this parameter (i.e. no dual role for obliquity and precession in the process of deglaciation).

In summary, the results for Scenario II (in which Max deglac is aligned with peak precession) are consistent with a dual role for precession and obliquity in deglaciation and the proposition that precession plays a more important role in the precise timing of deglacial onset (*5*), while obliquity is more important for the timing of Peak IG and Max inception. The equivalent is not true for Scenario III. Setting Max deglac to peak obliquity does not result in strong alignment of Max inception with respect to precession and implies that no relationship exists between precession and deglaciation.

We note that while our conclusion (that precession is more important than obliquity for the onset of deglaciation) appears to contradict that of ref (*7*), both studies find that mid-deglaciation (Max deglac in our case) is aligned (approximately) with maximum summer insolation as a function of both obliquity and precession. Moreover, ref (*7*) noted a negative relationship between the value of obliquity at the onset of termination and the duration of termination. We suggest this reflects the fact that deglaciations tend to be longer when the peak to peak offset between precession and obliquity is greatest. For example the precession peak associated with T5 commenced while obliquity was close to minimum (Fig. 3B). This resulted in a very long (protracted) deglacial interval, reflecting the large phase offset at that time. In contrast, the precession peak associated with T2 commenced while obliquity was relatively high (i.e. precession and obliquity were close to being in phase; Fig. 3A), resulting in a much shorter period of deglaciation.

5. Importance of latitude for the waxing and waning of northern ice sheets

The combined effects of obliquity and precession (as modulated by eccentricity) on insolation are typically quantified using a single metric for example June 21 (peak northern summer) intensity or some measure of integrated summer insolation at 65°N. However, the relative contribution of obliquity versus precession to any given insolation metric decreases significantly as one moves from higher to lower latitudes (*11*) (Fig. 5A). Consequently, use of a single metric at a fixed latitude may be inadequate for defining the forcing relevant to an ice sheet whose mean latitude varies with time. Our results underscore this issue because they require that the relative importance of obliquity versus precession varies throughout a glacial cycle. Specifically, while precession appears to be more important for melting back very large ice sheets from their maximum extent, obliquity is more important for the end of glacial retreat and the beginning of the next glacial cycle. Glacial inception must occur at high latitude sites (north of ~70°N) such as the Canadian Arctic Archipelago (*26*). In these regions the contribution of obliquity to calorific summer insolation significantly outweighs that of precession (Fig. 5A). As ice sheets develop, their mean latitude will migrate southwards, to latitudes where precession is more important, until they attain their full glacial maximum position. At this point (anywhere south of ~55°N) precession dominates variations in both peak summer intensity and calorific summer insolation, which can explain why the early stages of deglaciation are more strongly dependent on this parameter. Thereafter, as ice sheets decay, they retreat back toward higher latitudes where obliquity dominates (Fig. 5A).

Our inference (that precession is more important for the onset of deglaciation with obliquity more important for glacial inception) is supported by coupled climate-ice sheet model experiments. For example Abe-Ouchi et al. (*27*) demonstrated the sensitivity of very large ice sheets to even modest precession forcing at their southern margins, which could lead to their rapid disintegration during deglaciation. Vettoretti and Peltier (*28, 29*) emphasised the importance of obliquity for glacial inception, suggesting that occurrence of the Arctic insolation minimum in late spring, as a result of decreasing obliquity, led to delayed spring and summer snowmelt. Decreasing obliquity also increases the equator to pole insolation gradient during summer, which promotes northward moisture transport to feed growing icesheets (*29, 30*). On the other hand, other studies (*31, 32*) suggest that precession plays a more important role in glacial inception (as described in Section 7). In addition, conceptual models based on a limited number of tuneable parameters are able to simulate realistic timing of G-IG transitions using a single orbital solution (*33, 34*). Nevertheless, our results (Figs. 1, 2) clearly demonstrate the imprint of orbital phasing on deglaciation, which we contend is best explained by changes in the mean latitude and size of northern ice sheets and a corresponding change in their overall sensitivity to precession versus obliquity forcing.

So far, we have not considered the absolute magnitude of insolation forcing necessary for producing significant changes in ice sheet size. For example, the magnitude of precession forcing associated with T5 (leading to MIS 11) was small (a consequence of reduced eccentricity; Fig. 5B). And yet the magnitude of ice volume change across T5 was greater than terminations which experienced much larger variations in precession; hence, the 'Stage 11 problem' (*12, 35*). On the other hand, the vulnerability of very large ice sheets to even modest variations in precession might simply reflect their more southerly position (*27*) (Fig. 5B) or their inherent instability due to isostatic adjustments (*36*). In addition, feedbacks within the climate system play an important role in amplifying orbital forcing (*13, 37, 38*) and may therefore help to even out amplitude variations. For example, millennial-scale oscillations in ocean circulation and concomitant release of CO_2 during the early stages of termination can contribute to global warming at these times (*17, 39*). When ice sheets are particularly large (e.g. during MIS 12) it is possible that such feedbacks become substantial enough to compensate for potentially weaker precession forcing. Conversely, equivalent activity during glacial development may actually help to cool the deep ocean and provide additional storage capacity for lowering atmospheric CO_2 (*16, 38, 40*) (an essential aspect of glacial inception (*31*)).

It should be acknowledged that while our discussion has focussed on northern hemisphere ice sheet variability, fluctuations of the Antarctic ice sheet could account for a significant proportion (up to ~15%) of G-IG ice volume change (*41, 42*). We do not have a complete record of Antarctic ice sheet variability, but continuous temperature records do exist (*43, 44*). In Figure S7 we show a morphological comparison of the Antarctic temperature record (AAT) and the LR04 benthic stack over the past 800kyr. We observe a high degree of similarity ($R^2 = 0.93$) across deglaciations, implying (to first order) a common forcing.

Previous explanations of why Antarctic variability might resemble northern hemisphere insolation (which is counterintuitive, given that the effects of precession are out of phase between the hemispheres (*45*)) have relied on interhemispheric 'bridges' such as sea level and atmospheric CO_2 (*13, 46*). Alternatively, it has been suggested that southern hemisphere summer duration (which varies in phase with northern summer intensity as a function of precession) could explain the similarity (*47*). On the other hand, our explanation for the shift in influence

from precession to obliquity across (northern) deglaciation relies on a substantial change in the latitudinal distribution of ice, which is unlikely across Antarctica. Instead, we propose that precession could trigger the onset of deglacial Antarctic warming through heat redistribution associated with a substantial weakening of the Atlantic Meridional Overturning Circulation (AMOC) that might result from intensified summer melting of northern ice sheets (*37, 48-50*) and which in turn might be amplified by enhanced stratification of the glacial deep ocean (*39*). Notably, such an explanation could explain the observation of a southern lead at orbital timescales (*12, 51*), which would reflect the fact that deglacial warming across northern high latitudes is delayed by the same AMOC perturbations responsible for early warming in the south (*52, 53*).

An increase in the influence of obliquity towards the end of deglaciation in both hemispheres is more straightforward to explain thanks to the globally symmetric effects of obliquity.

6. Precession, obliquity and eccentricity combine to produce ~100kyr glacial cycles

The dominant ~100kyr period of mid/late Pleistocene G-IG cyclicity (*1*) is problematic because direct orbital forcing at this period (via eccentricity) is weak (*12*). Most recent studies have concluded that the large magnitude of glacial terminations must involve forcing by some combination of precession and/or obliquity with additional feedbacks internal to the climate system (*37*) and our results shed light on how these parameters combine to produce the observed morphology of deglacial/interglacial periods. However, there remains the question as to why glacial cycles should endure for so long and why they have such a strong link to eccentricity (*14*) (Fig. 5B). Raymo (*2*) suggested that an extended interval of low amplitude precession forcing (under the influence of low eccentricity) would allow the build-up of large continental ice sheets by enabling them to expand southwards until they reached some critical size, after which they would become susceptible to even modest insolation forcing. Accordingly, most successful models of G-IG variability (*8, 9, 13, 34, 54*) incorporate a critical ice volume threshold (V_{crit}), beyond which termination becomes possible/inevitable.

Our results provide empirical constraints for predicting the occurrence and duration of glacial terminations and interglacials since the Mid Pleistocene Transition (MPT i.e. the 100kyr world; Fig. 6). As stated, the set of precession peaks associated with Max deglac for each termination of the past 1Myr is identical for all of the $\delta^{18}O$ records analysed here (Fig. S2). Furthermore, each of those peaks was aligned with average to high values of obliquity (Fig. 1D, E), which implies that obliquity was rising as peak summer intensity began increasing as a function of precession (see orange symbols in Fig. 1D, E). This is true for all terminations except T8, whose precession peak begins ~724ka, about 1kyr before the next minimum in obliquity (Fig. 1D, E) and therefore about 2kyr before obliquity starts to rise. Notably, according to 3 out of 4 $\delta^{18}O$ records, the measured offset between Onset deglac and Max deglac associated with T8 is shorter than the average (Fig. S2). This is particularly noticeable for LR04 (Fig. 1C) and we speculate that this is due to the relatively late (~2kyr) rise in obliquity associated with that termination. We therefore consider precession peaks as candidates for termination if they begin while obliquity is rising or begins rising within 2kyr of the turning point in precession (to accommodate the case of T8). Thus the onset of deglaciation occurred only when summers were warming through the reinforcing (dual) effects of obliquity and precession (see also results in Fig. 4). In Figure 6H we plot all such 'candidate' precession peaks of the past 1Myr.

Significantly the subset of candidate precession peaks resulting in termination over the past 900kyr is precisely those that directly followed a minimum in eccentricity (Fig. 6H; note that the eccentricity minimum ~373Ka coincided precisely with a candidate precession peak but the following candidate peak was the terminating peak). For context, there have been 45 precession peaks since 0.95Ma, of which 25 (~1/2) were candidate peaks and just 10 (1/4.5) were associated with glacial termination (i.e. on average terminations were separated by 4.5 precession cycles, ~95kyr).

Glacial termination therefore occurs with the first candidate precession peak following each minimum in eccentricity. This might suggest that V_{crit} is attained as soon as eccentricity reaches its minimum, after which the next candidate peak in precession triggers deglaciation. However, we note that in many cases, one or more non-candidate precession peaks occurred within the interval between the minimum in eccentricity and the terminating precession peak. Since non-candidate precession peaks are (by definition) those that align with low obliquity, continued ice growth during these intervals might also be critical for attainment of V_{crit} prior to termination (*13*). In any case, our observations allow us to construct an algorithm capable of predicting the occurrence of all major glacial terminations over the past 900kyr, based simply on the subset of candidate precession peaks that follow directly after minima in eccentricity (Fig. 6H). In Figure 6D we also incorporate predictions for the key points (Peak IG and Max inception), based on the phasing of precession versus obliquity during termination.

The results compare well with those obtained from a simple thresholding approach used to predict interglacial stages of the past 1Myr (*10*) (Fig. 6I), with three exceptions: In two cases, our algorithm does not predict the transitions into marine isotope substages 7c or 15a. While these events were aligned with candidate peaks (Fig. 6G), they were relatively short in duration with respect to the phasing of precession versus obliquity (Fig. 2C, D) and do not fall within the set of major terminations. Notably though, they occurred when the amplitude of precession forcing was particularly large (thanks to high eccentricity). We therefore consider MIS 7c and 15a as anomalously warm substages, analogous to MIS 5a and 9a (Fig 6G) but of larger amplitude thanks to the direct influence of eccentricity on precession. In the third case, T6 was a protracted (2-step) termination (*55*), resulting in the delayed attainment of full interglacial conditions (MIS 13a) according to the prediction of (*10*). The preceding glacial (MIS 14) was particularly weak (*56*) and the smaller size of ice sheets (Fig. 6G) might explain the weaker response to orbital forcing associated with the first step (T6). The second step (T6a) was also aligned with a candidate precession peak and its duration (relative to orbital phasing) was in line with all other major terminations (Fig. 2C, D). Thus the full deglaciation from MIS 14 into MIS 13a could be considered as 2 distinct deglacial events, each following the pattern of other major terminations of the past 900kyr.

Our simple rules for predicting the occurrence of terminating precession peaks do not hold prior to 0.9Ma (Figs. 6, S8). Notably, this was during the Mid Pleistocene Transition (~1.2 to 0.8Ma (*57-61*)) before which glacial cycles had a period of ~41kyr, similar to that of obliquity. At that time, according to the records and age models used here, deglacial transitions were also more closely aligned with candidate precession peaks (i.e. those that commenced while obliquity was increasing) than with non-candidate peaks, with almost all candidate peaks being associated with a deglacial event (Fig. S8), which is in contrast to the 100kyr world (Fig. 6). This does not necessarily imply that precession was critical for deglacial transitions before the MPT because our definition of a candidate precession peak is one that coincides with moderate to high

obliquity (which therefore could be solely responsible for pre-MPT deglaciations). On the other hand, it does imply that eccentricity had little influence on the duration of glacial periods prior to the MPT. We might therefore explain the change from ~41 to ~100kyr glacial periodicity across the MPT as resulting from the increasing ability of ice sheets to grow and/or expand southwards quickly enough to escape the influence of obliquity (e.g. by secular global cooling, changes in glacial erosion or an increase in moisture transport associated with the Atlantic Inflow (*10, 11, 59, 60, 62, 63*)), while simultaneously escaping the influence of precession thanks to decreasing eccentricity (*2, 54*). Eventually though, ice sheets would reach a latitude and size where even a modest change in precession could trigger glacial termination (*27, 36*). Thus the MPT saw the introduction of a dependency on eccentricity, but crucially this was not associated with maxima in eccentricity but rather minima, providing the necessary time required to grow very large ice sheets (*2, 10, 34, 54*).

Finally, we note that ~100kyr periodicity has also been observed for glacial cycles during earlier epochs, for example the early to mid Miocene (*64, 65*). At that time, continental ice was most likely confined to Antarctica (*66*) and while the mechanisms we invoke to explain ~100kyr periodicity during the Pleistocene are focused on northern hemisphere processes, future work should investigate whether or not equivalent mechanisms involving the Antarctic ice sheet could be called upon during earlier intervals. Notably, the potential importance of millennial-scale variability and its possible interactions with orbital timescale changes has been invoked for the Miocene (*67*) as well as the mid to late Pleistocene (*37, 38*).

7. The natural future of Earth's climate

Our results suggest that the succession and duration of deglacial/interglacial events since the MPT might be largely determined by the relative phasing of precession, obliquity and eccentricity (Fig. 6D). This deterministic quality (previously inferred from theoretical/model-based approaches (*9, 68, 69*)) provides an opportunity to hypothesise about the possible future of Earth's climate. There has been considerable discussion as to when the next glacial inception might occur (*29, 31, 32, 70*). Most studies agree that glacial inception results from some critical combination of orbital configuration and the atmospheric concentration of CO_2 and there is little debate that while CO_2 levels continue to rise there is almost no chance of a return to glacial conditions (*29, 31*). Notwithstanding, it is important to understand the natural variability of climate and how this might play out if and when the anthropogenic input of CO_2 is reduced to pre-industrial levels. Classical orbital theory predicts that glacial inception should occur when northern hemisphere summers are cool enough to allow perennial snow to accumulate, through some combination of low obliquity and a positive precession parameter (when northern summer aligns with aphelion). Orbital eccentricity (the circularity of Earth's orbit around the Sun) is currently low ($e \approx 0.017$ compared with a maximum of ~0.58), resulting in very modest variations in precession (Figs. 6, 7). Consequently, model predictions based on the intensity of peak summer insolation at 65°N (a signal dominated by precession) tend to escape inception for tens of thousands of years into the future even in the hypothetical absence of anthropogenic CO_2 (*31, 32*). On the other hand, models that emphasize the importance of obliquity (over precession) in the process of inception (*28, 29*) predict glacial inception as early as 10kyr from now (with CO_2 held at 260ppmv).

Our results also suggest that glacial inception depends mainly on the phase of obliquity, and moreover that the duration between Peak IG and Max inception is rather invariant (Fig. 2B) and therefore relatively insensitive to the amplitude of precession forcing. For example, eccentricity was also low across T5 (as discussed above) and although MIS 11 was long, it fell within the natural set of mid to late Pleistocene interglacials whose durations were dictated by the phasing of precession versus obliquity during deglaciation (i.e. it was not exceptional; Fig. 7A). Conversely, MIS 7e was relatively short and occurred when eccentricity was high, but its short duration could again be predicted simply from the negative peak-to-peak offset between precession and obliquity across T3 (Fig. 7B). MIS 19 (following T9), which is often taken as an analogue for our current interglacial (MIS 1) because it experienced similar variations in insolation (*70*) (i.e. low eccentricity with precession and obliquity approximately in-phase during deglaciation), also had a duration in keeping with predictions based on orbital phasing rather than eccentricity (Fig. 7C).

We therefore calculate when the next maximum in glacial inception might occur (ignoring the effects of anthropogenic CO_2) based on the phasing of precession versus obliquity during the last deglaciation (T1). According to the various records we employ, benthic $\delta^{18}O$ has continued to decrease throughout the Holocene, which results in an age of zero being assigned to MIS 1 Peak IG (Fig. 7D) although we cannot know whether or not this the actual minimum because there is no record of the future. We therefore predict the timing of MIS 1 Peak IG from the empirical relationships shown in Figure 2 (and S3) while omitting T1. We set Max deglac for each record either to the age of Max deglac on LR04 (which is based on ^{14}C dating (*19*); Set L in Fig. 7D) or the precession peak ~11ka (Set P in Fig. 7D) (*16*). We then use the calculated values of Max deglac minus Peak IG to estimate the age of Max inception. We obtain an age of -0.1±1.8kyr (2σ) for MIS 1 Peak IG and -7.7±3.4kyr (2σ) for the next Max inception. Thus we estimate that, if not for the effects of increasing CO_2, glacial inception would reach a maximum rate within the next 11kyr, as obliquity decreases towards its next minimum.

Our extrapolation also suggests that the next interglacial event would begin ~66kyr from now (following a glacial cycle spanning 4 precession peaks; Fig. 6D). The same timing is predicted by the simple rules outlined in ref (*10*) (Fig. 6). On the other hand, while atmospheric CO_2 remains above pre-industrial levels it is highly unlikely that glacial inception will occur (*29, 31, 71*), in which case the pattern of future interglacials will be very different from the predictions made here.

References and Notes

1. J. D. Hays, J. Imbrie, N. J. Shackleton, Variations in the Earth's orbit: Pacemaker of the Ice Ages. *Science* **194**, 1121-1132 (1976).
2. M. E. Raymo, The timing of major climate terminations. *Paleoceanography* **12**, 577-585 (1997).
3. A. J. Ridgwell, A. J. Watson, M. E. Raymo, Is the spectral signature of the 100 kyr glacial cycle consistent with a Milankovitch origin? *Paleoceanography* **14**, 437-440 (1999).

4. H. Cheng, R. L. Edwards, A. Sinha, C. Spötl, L. Yi, S. Chen, M. Kelly, G. Kathayat, X. Wang, X. Li, The Asian monsoon over the past 640,000 years and ice age terminations. *Nature* **534**, 640-646 (2016).
5. B. Hobart, L. E. Lisiecki, D. Rand, T. Lee, C. E. Lawrence, Late Pleistocene 100-kyr glacial cycles paced by precession forcing of summer insolation. *Nature Geoscience* **16**, 717-722 (2023).
6. P. Huybers, C. Wunsch, Obliquity pacing of the late Pleistocene glacial terminations. *Nature* **434**, 491-494 (2005).
7. P. Bajo, R. N. Drysdale, J. D. Woodhead, J. C. Hellstrom, D. Hodell, P. Ferretti, A. H. Voelker, G. Zanchetta, T. Rodrigues, E. Wolff, Persistent influence of obliquity on ice age terminations since the Middle Pleistocene transition. *Science* **367**, 1235-1239 (2020).
8. P. Huybers, Combined obliquity and precession pacing of late Pleistocene deglaciations. *Nature* **480**, 229-232 (2011).
9. F. Parrenin, D. Paillard, Terminations VI and VIII (~ 530 and~ 720 kyr BP) tell us the importance of obliquity and precession in the triggering of deglaciations. *Climate of the Past* **8**, 2031-2037 (2012).
10. P. C. Tzedakis, M. Crucifix, T. Mitsui, E. W. Wolff, A simple rule to determine which insolation cycles lead to interglacials. *Nature* **542**, 427-432 (2017).
11. S. Barker, A. Starr, J. v. d. Lubbe, A. Doughty, G. Knorr, S. Conn, S. Lordsmith, L. Owen, A. Nederbragt, S. Hemming, I. Hall, L. Levay, Persistent influence of precession on northern ice sheet variability since the early Pleistocene. *Science* **376**, 961-967 (2022) doi: 10.1126/science.abm4033.
12. J. Imbrie, A. Berger, E. A. Boyle, S. C. Clemens, A. Duffy, W. R. Howard, G. Kukla, J. Kutzbach, D. G. Martinson, A. McIntyre, A. C. Mix, B. Molfino, J. J. Morley, L. C. Peterson, N. G. Pisias, W. L. Prell, M. E. Raymo, N. J. Shackleton, J. R. Toggweiler, On the structure and origin of major glaciation cycles 2. the 100,000-year cycle. *Paleoceanography* **8**, 699-735 (1993).
13. A. Ganopolski, Toward generalized Milankovitch theory (GMT). *Climate of the Past* **20**, 151-185 (2024).
14. L. E. Lisiecki, Links between eccentricity forcing and the 100,000-year glacial cycle. *Nature geoscience* **3**, 349-352 (2010).
15. H. Elderfield, P. Ferretti, M. Greaves, S. Crowhurst, I. N. McCave, D. Hodell, A. M. Piotrowski, Evolution of Ocean Temperature and Ice Volume Through the Mid-Pleistocene Climate Transition. *Science* **337**, 704-709 (2012).
16. See Supplementary Materials.
17. D. Baggenstos, M. Häberli, J. Schmitt, S. A. Shackleton, B. Birner, J. P. Severinghaus, T. Kellerhals, H. Fischer, Earth's radiative imbalance from the Last Glacial Maximum to the present. *Proceedings of the National Academy of Sciences* **116**, 14881-14886 (2019).
18. S. Shackleton, A. Seltzer, D. Baggenstos, L. E. Lisiecki, Benthic δ18O records Earth's energy imbalance. *Nature Geoscience* **16**, 797-802 (2023).
19. L. E. Lisiecki, M. E. Raymo, A Pliocene-Pleistocene stack of 57 globally distributed benthic $\delta^{18}O$ records. *Paleoceanography* **20**, DOI:10.1029/2004PA001071 (2005).
20. P. Huybers, C. Wunsch, A depth-derived Pleistocene age model: Uncertainty estimates, sedimentation variability, and nonlinear climate change. *Paleoceanography* **19**, (2004).

21. P. Huybers, Glacial variability over the last two million years: an extended depth-derived agemodel, continuous obliquity pacing, and the Pleistocene progression. *Quaternary Science Reviews* **26**, 37-55 (2007).
22. PIGS_of_PAGES, Interglacials of the last 800,000 years. *Reviews of Geophysics* **54**, 162-219 (2016).
23. G. Roe, In defense of Milankovitch. *Geophysical Research Letters* **33**, (2006) 10.1029/2006GL027817.
24. N. J. Shackleton, N. D. Opdyke, Oxygen isotope and palaeomagnetic stratigraphy of Equatorial Pacific core V28-238: Oxygen isotope temperatures and ice volumes on a 105 year and 106 year scale. *Quaternary Research* **3**, 39-55 (1973).
25. P. C. Tzedakis, E. Wolff, L. Skinner, V. Brovkin, D. Hodell, J. F. McManus, D. Raynaud, Can we predict the duration of an interglacial? *Climate of the Past* **8**, 1473-1485 (2012).
26. P. Clark, J. Clague, B. B. Curry, A. Dreimanis, S. Hicock, G. Miller, G. Berger, N. Eyles, M. Lamothe, B. Miller, Initiation and development of the Laurentide and Cordilleran ice sheets following the last interglaciation. *Quaternary Science Reviews* **12**, 79-114 (1993).
27. A. Abe-Ouchi, F. Saito, K. Kawamura, M. E. Raymo, J. i. Okuno, K. Takahashi, H. Blatter, Insolation-driven 100,000-year glacial cycles and hysteresis of ice-sheet volume. *Nature* **500**, 190-193 (2013).
28. G. Vettoretti, W. R. Peltier, Sensitivity of glacial inception to orbital and greenhouse gas climate forcing. *Quaternary Science Reviews* **23**, 499-519 (2004).
29. G. Vettoretti, W. Peltier, The impact of insolation, greenhouse gas forcing and ocean circulation changes on glacial inception. *The Holocene* **21**, 803-817 (2011).
30. M. E. Raymo, K. Nisancioglu, The 41 kyr world: Milankovitch's other unsolved mystery. *Paleoceanography* **18**, (2003) 10.1029/2002PA000791.
31. A. Ganopolski, R. Winkelmann, H. J. Schellnhuber, Critical insolation–CO2 relation for diagnosing past and future glacial inception. *Nature* **529**, 200-203 (2016).
32. A. Berger, M. F. Loutre, An exceptionally long interglacial ahead? *Science* **297**, 1287-1288 (2002).
33. F. Parrenin, D. Paillard, Amplitude and phase of glacial cycles from a conceptual model. *Earth and Planetary Science Letters* **214**, 243-250 (2003).
34. E. Legrain, F. Parrenin, E. Capron, A gradual change is more likely to have caused the mid-pleistocene transition than an abrupt event. *Communications Earth & Environment* **4**, 90 (2023).
35. P. C. Tzedakis, D. A. Hodell, C. Nehrbass-Ahles, T. Mitsui, E. W. Wolff, Marine isotope stage 11c: An unusual interglacial. *Quaternary Science Reviews* **284**, 107493 (2022).
36. D. R. MacAyeal, A Catastrophe Model of the Paleoclimate. *Journal of Glaciology* **24**, 245-257 (1979).
37. S. Barker, G. Knorr, Millennial scale feedbacks determine the shape and rapidity of glacial termination. *Nature Communications* **12**, 2273 (2021) 10.1038/s41467-021-22388-6.
38. S. Barker, G. Knorr, A Systematic Role for Extreme Ocean-Atmosphere Oscillations in the Development of Glacial Conditions Since the Mid Pleistocene Transition. *Paleoceanography and Paleoclimatology* **38**, (2023) 10.1029/2023PA004690.
39. G. Knorr, S. Barker, X. Zhang, G. Lohmann, X. Gong, P. Gierz, C. Stepanek, L. B. Stap, A salty deep ocean as a prerequisite for glacial termination. *Nature Geoscience* **14**, 930-936 (2021).

40. S. Shackleton, J. A. Menking, E. Brook, C. Buizert, M. N. Dyonisius, V. V. Petrenko, D. Baggenstos, J. P. Severinghaus, Evolution of mean ocean temperature in Marine Isotope Stage 4. *Climate of the Past* **17**, 2273-2289 (2021).
41. R. M. DeConto, D. Pollard, Contribution of Antarctica to past and future sea-level rise. *Nature* **531**, 591-597 (2016).
42. N. R. Golledge, R. H. Levy, R. M. McKay, C. J. Fogwill, D. A. White, A. G. Graham, J. A. Smith, C.-D. Hillenbrand, K. J. Licht, G. H. Denton, Glaciology and geological signature of the Last Glacial Maximum Antarctic ice sheet. *Quaternary Science Reviews* **78**, 225-247 (2013).
43. J. Jouzel, V. Masson-Delmotte, O. Cattani, G. Dreyfus, S. Falourd, G. Hoffmann, B. Minster, J. Nouet, J. M. Barnola, J. Chappellaz, H. Fischer, J. C. Gallet, S. Johnsen, M. Leuenberger, L. Loulergue, D. Luethi, H. Oerter, F. Parrenin, G. Raisbeck, D. Raynaud, A. Schilt, J. Schwander, E. Selmo, R. Souchez, R. Spahni, B. Stauffer, J. P. Steffensen, B. Stenni, T. F. Stocker, J. L. Tison, M. Werner, E. W. Wolff, Orbital and millennial Antarctic climate variability over the past 800,000 years. *Science* **317**, 793-796 (2007).
44. F. Parrenin, V. Masson-Delmotte, P. Kohler, D. Raynaud, D. Paillard, J. Schwander, C. Barbante, A. l. Landais, A. Wegner, J. Jouzel, Synchronous change of atmospheric CO_2 and Antarctic temperature during the last deglacial warming. *Science* **339**, 1060-1063 (2013).
45. J. H. Mercer, in *Climate Processes and Climate Sensitivity,* J. E. Hansen, Takahash.T, Eds. (American Geophysical Union, 1984), vol. 29, pp. 307-313.
46. T. T. Barrows, S. Juggins, P. De Deckker, E. Calvo, C. Pelejero, Long-term sea surface temperature and climate change in the Australian–New Zealand region. *Paleoceanography* **22**, (2007).
47. P. Huybers, G. Denton, Antarctic temperature at orbital timescales controlled by local summer duration. *Nature Geoscience* **1**, 787-792 (2008).
48. S. Barker, P. Diz, M. J. Vautravers, J. Pike, G. Knorr, I. R. Hall, W. S. Broecker, Interhemispheric Atlantic seesaw response during the last deglaciation. *Nature* **457**, 1097-1102 (2009).
49. E. W. Wolff, H. Fischer, R. Rothlisberger, Glacial terminations as southern warmings without northern control. *Nature Geoscience* **2**, 206-209 (2009).
50. G. H. Denton, R. F. Anderson, J. R. Toggweiler, R. L. Edwards, J. M. Schaefer, A. E. Putnam, The Last Glacial Termination. *Science* **328**, 1652-1656 (2010).
51. C. Wunsch, Greenland - Antarctic phase relations and millennial time-scale climate fluctuations in the Greenland ice-cores. *Quaternary Science Reviews* **22**, 1631-1646 (2003).
52. S. Barker, G. Knorr, R. L. Edwards, F. Parrenin, A. E. Putnam, L. C. Skinner, E. Wolff, M. Ziegler, 800,000 years of abrupt climate variability. *Science* **334**, 347-351 (2011).
53. J. D. Shakun, P. U. Clark, F. He, S. A. Marcott, A. C. Mix, Z. Liu, B. Otto-Bliesner, A. Schmittner, E. Bard, Global warming preceded by increasing carbon dioxide concentrations during the last deglaciation. *Nature* **484**, 49-54 (2012).
54. D. Paillard, The timing of Pleistocene glaciations from a simple multiple-state climate model. *Nature* **391**, 378 (1998).
55. S. Barker, G. Knorr, S. Conn, S. Lordsmith, D. Newman, D. Thornalley, Early interglacial legacy of deglacial climate instability. *Paleoceanography and Paleoclimatology*, (2019) 10.1029/2019PA003661.
56. N. Lang, E. W. Wolff, Interglacial and glacial variability from the last 800 ka in marine, ice and terrestrial archives. *Climate of the Past* **7**, 361 (2011).

57. N. J. Shackleton, N. D. Opdyke, Oxygen-isotope and paleomagnetic stratigraphy of Pacific core V28-239 late Pliocene to latest Pleistocene. (1976).
58. N. G. Pisias, T. Moore Jr, The evolution of Pleistocene climate: a time series approach. *Earth and Planetary Science Letters* **52**, 450-458 (1981).
59. P. U. Clark, D. Archer, D. Pollard, J. D. Blum, J. A. Rial, V. Brovkin, A. C. Mix, N. G. Pisias, M. Roy, The middle Pleistocene transition: characteristics. mechanisms, and implications for long-term changes in atmospheric PCO2. *Quaternary Science Reviews* **25**, 3150-3184 (2006).
60. S. Barker, X. Zhang, L. Jonkers, S. Lordsmith, S. Conn, G. Knorr, Strengthening Atlantic Inflow across the Mid-Pleistocene Transition. *Paleoceanography and Paleoclimatology*, (2021) 10.1029/2020PA004200.
61. P. U. Clark, D. Pollard, Origin of the middle Pleistocene transition by ice sheet erosion of regolith. *Paleoceanography* **13**, 1-9 (1998).
62. W. H. Berger, E. Jansen, in *The polar oceans and their role in shaping the global environment*. (AGU, 1994), pp. 295-311.
63. E. L. McClymont, S. M. Sosdian, A. Rosell-Melé, Y. Rosenthal, Pleistocene sea-surface temperature evolution: Early cooling, delayed glacial intensification, and implications for the mid-Pleistocene climate transition. *Earth-Science Reviews* **123**, 173-193 (2013).
64. D. Liebrand, L. Lourens, D. Hodell, B. De Boer, R. Van de Wal, H. Pälike, Antarctic ice sheet and oceanographic response to eccentricity forcing during the early Miocene. *Climate of the Past* **7**, 869-880 (2011).
65. A. Holbourn, W. Kuhnt, K. G. Kochhann, N. Andersen, K. Sebastian Meier, Global perturbation of the carbon cycle at the onset of the Miocene Climatic Optimum. *Geology* **43**, 123-126 (2015).
66. J. Zachos, M. Pagani, L. Sloan, E. Thomas, K. Billups, Trends, rhythms, and aberrations in global climate 65 Ma to present. *Science* **292**, 686-693 (2001).
67. N. B. Sullivan, S. R. Meyers, R. H. Levy, R. M. McKay, N. R. Golledge, G. Cortese, Millennial-scale variability of the Antarctic ice sheet during the early Miocene. *Proceedings of the National Academy of Sciences* **120**, e2304152120 (2023).
68. M. Willeit, A. Ganopolski, R. Calov, V. Brovkin, Mid-Pleistocene transition in glacial cycles explained by declining CO2 and regolith removal. *Science Advances* **5**, eaav7337 (2019).
69. S. R. Meyers, L. A. Hinnov, Northern Hemisphere glaciation and the evolution of Plio-Pleistocene climate noise. *Paleoceanography* **25**, (2010).
70. P. C. Tzedakis, J. Channell, D. Hodell, H. Kleiven, L. Skinner, Determining the natural length of the current interglacial. *Nature Geoscience* **5**, 138-141 (2012).
71. D. Archer, A. Ganopolski, A movable trigger: Fossil fuel CO2 and the onset of the next glaciation. *Geochemistry Geophysics Geosystems* **6**, (2005).
72. A. Berger, M. F. Loutre, Insolation Values for the Climate of the Last 10 Million Years. *Quaternary Science Reviews* **10**, 297-317 (1991).
73. M. Crucifix, Palinsol: insolation for palaeoclimate studies, R package version 0.93. https://bitbucket.org/mcrucifix/insol (2016).
74. C. Waelbroeck, J. C. Duplessy, E. Michel, L. Labeyrie, D. Paillard, J. Duprat, The timing of the last deglaciation in North Atlantic climate records. *Nature* **412**, 724-727 (2001).
75. N. J. Shackleton, M. A. Hall, E. Vincent, Phase relationships between millennial-scale events 64,000- 24,000 years ago. *Paleoceanography* **15**, 565-569 (2000).

76. R. B. Alley, E. J. Brook, S. Anandakrishnan, A northern lead in the orbital band: north-south phasing of Ice-Age events. *Quaternary Science Reviews* **21**, 431-441 (2002).
77. A. Schmittner, O. A. Saenko, A. J. Weaver, Coupling of the hemispheres in observations and simulations of glacial climate change. *Quaternary Science Reviews* **22**, 659-671 (2003).
78. S. Barker, G. Knorr, Antarctic climate signature in the Greenland ice core record. *Proceedings of the National Academy of Sciences of the United States of America* **104**, 17278-17282 (2007).
79. L. Skinner, N. Shackleton, Deconstructing Terminations I and II: revisiting the glacioeustatic paradigm based on deep-water temperature estimates. *Quaternary Science Reviews* **25**, 3312-3321 (2006).
80. D. M. Sigman, M. P. Hain, G. H. Haug, The polar ocean and glacial cycles in atmospheric CO_2 concentration. *Nature* **466**, 47-55 (2010).
81. J. F. Adkins, The role of deep ocean circulation in setting glacial climates. *Paleoceanography* **28**, 539-561 (2013).
82. P. Berens, CircStat: a MATLAB toolbox for circular statistics. *J Stat Softw* **31**, 1-21 (2009).
83. J. V. Stern, L. E. Lisiecki, Termination 1 timing in radiocarbon-dated regional benthic δ18O stacks. *Paleoceanography* **29**, 1127-1142 (2014).
84. B. Bereiter, S. Shackleton, D. Baggenstos, K. Kawamura, J. Severinghaus, Mean global ocean temperatures during the last glacial transition. *Nature* **553**, 39 (2018).
85. K. Lambeck, H. Rouby, A. Purcell, Y. Sun, M. Sambridge, Sea level and global ice volumes from the Last Glacial Maximum to the Holocene. *Proceedings of the National Academy of Sciences* **111**, 15296-15303 (2014).
86. L. Bazin, A. Landais, B. Lemieux-Dudon, H. Toyé Mahamadou Kele, D. Veres, F. Parrenin, P. Martinerie, C. Ritz, E. Capron, V. Lipenkov, An optimized multi-proxy, multi-site Antarctic ice and gas orbital chronology (AICC2012): 120-800 ka. *Climate of the Past* **9**, 1715-1731 (2013).
87. D. Veres, L. Bazin, A. Landais, H. ToyÃ© Mahamadou Kele, B. Lemieux-Dudon, F. Parrenin, P. Martinerie, E. Blayo, T. Blunier, E. Capron, The Antarctic ice core chronology (AICC2012): an optimized multi-parameter and multi-site dating approach for the last 120 thousand years. *Climate of the Past Discussions* **8**, 6011-6049 (2012).

Acknowledgments: We thank M. Crucifix for assistance with palinsol. This is Cardiff EARTH CRediT contribution 26. **Author contributions:** Conceptualization: SB, LEL, GK, PCT; Methodology: SB; Investigation: SB; Visualization: SB; Writing – original draft: SB, LEL, GK, PCT ; Writing – review & editing: SB, LEL, GK, SN, PCT. **Competing interests:** Authors declare that they have no competing interests. **Data and materials availability:** All data used in this study were published previously and readers are referred to the references listed within supplementary materials. All analyses used in this study are described in the supplementary materials.

Supplementary Materials

Materials and Methods

Figs. S1 to S9

Tables S1 to S2

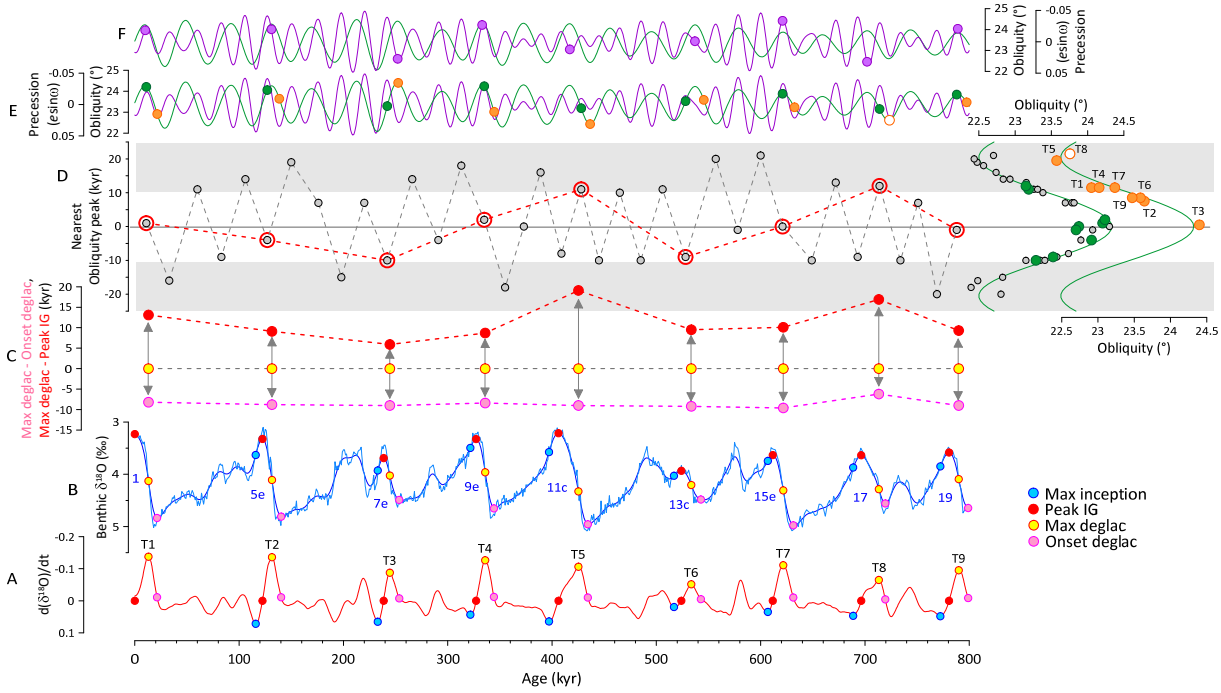

Fig. 1. Deglacial morphology and the phasing of obliquity versus precession. (A, B) The LR04 benthic $\delta^{18}O$ stack (B) and its first derivative (A), used to identify the key points as described in main text (coloured symbols). Terminations are numbered T1-T9, MIS numbers in blue. (C) Calculated temporal offsets: Max deglac minus Onset deglac (pink symbols), Max deglac minus Peak IG (red). Variability in the duration of deglaciation (double-headed grey arrows) is dominated by changes in the offset between Max deglac and Peak IG. (D) Precession peaks plotted versus their temporal offset to the closest obliquity peak in each case. Large red symbols (joined by dashed lines) are those precession peaks that are closest to Max deglac in each case. All of these coincide with moderate to high values of obliquity as demonstrated by green symbols to right. Also plotted is the value of obliquity (orange symbols) associated with the beginning of each terminal precession peak (i.e. when the precession parameter shifts from increasing to decreasing; see also Part E and discussion in Section 6). (E) Precession and obliquity (*72*) over last 1Myr. Green symbols highlight value of obliquity at each terminal precession peak, orange symbols highlight phase of obliquity at the beginning of each terminal precession peak (increasing in all cases except T8, which starts to increase within 2kyr; see text). (F) Same as E but purple symbols reflect value of precession parameter for the closest obliquity maximum to each Max deglaciation (no systematic pattern is observed cf. Fig. S6E3).

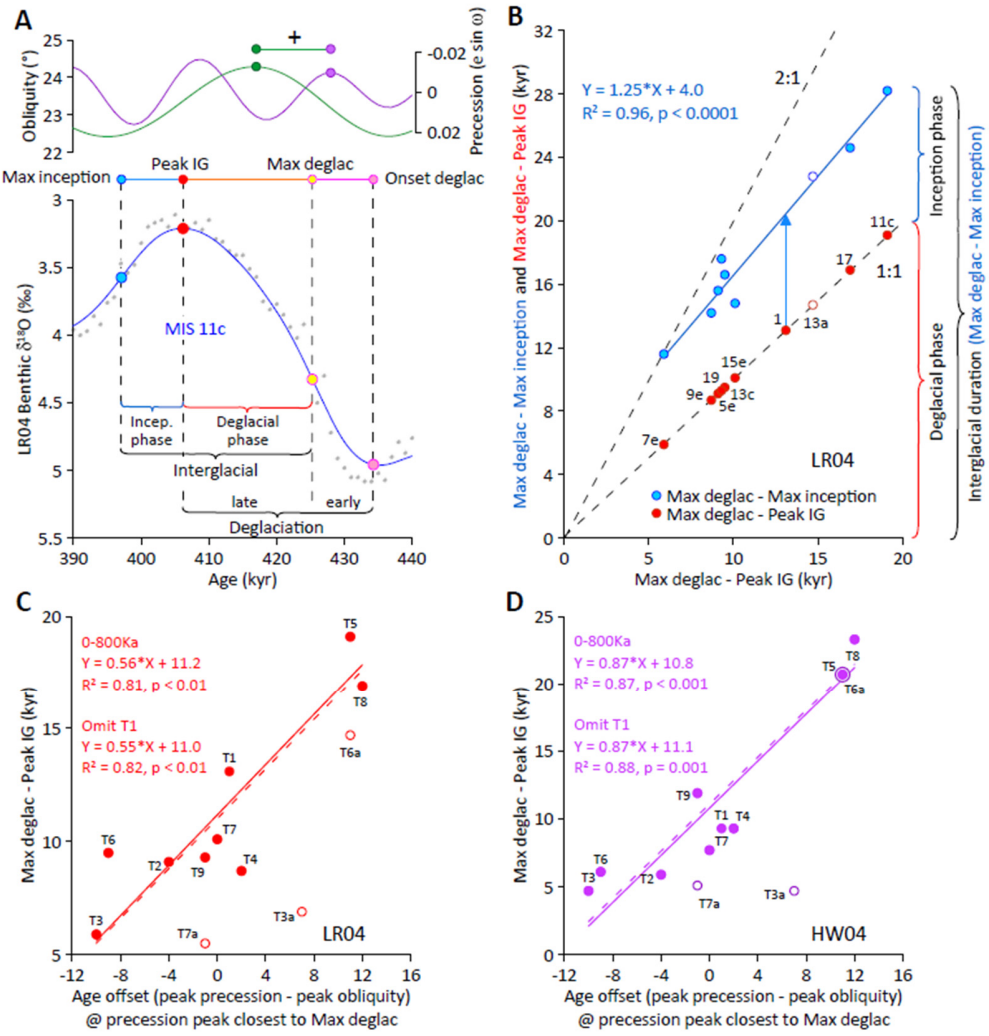

Fig. 2. Orbital phasing determines the duration of deglaciation. (A) Detail of interglacial anatomy for MIS 11c (associated with T5). Each interglacial is divided into a deglaciation phase (i.e. late deglaciation, between Max deglac and Peak IG) and a phase of glacial inception (between Peak IG and Max inception). Upper curves of precession and obliquity highlight offset between their respective peaks (positive in this case). (B) Correlation between Max deglac minus Max inception (interglacial duration) versus Max deglac minus Peak IG (deglacial phase; numbers are MIS). The inception phase is relatively invariant as compared with that of the deglacial phase, giving rise to increasingly asymmetric interglacials as their duration increases (see also Fig. 7A-C). The high value of R^2 implies that time to Max inception might be predicted for MIS 1 if we know the offset between Max deglac and Peak IG (blue arrow; see also Fig. 7D). (C, D) Correlation between Max deglac minus Peak IG and peak precession minus peak obliquity for LR04 and HW04. Dashed fits omit T1. Note that T3a, T6a/MIS13a and T7a (hollow symbols) are not included in the correlations (see discussion in Section 6). Equivalent correlations for other records are given in Figs. S3, S4.

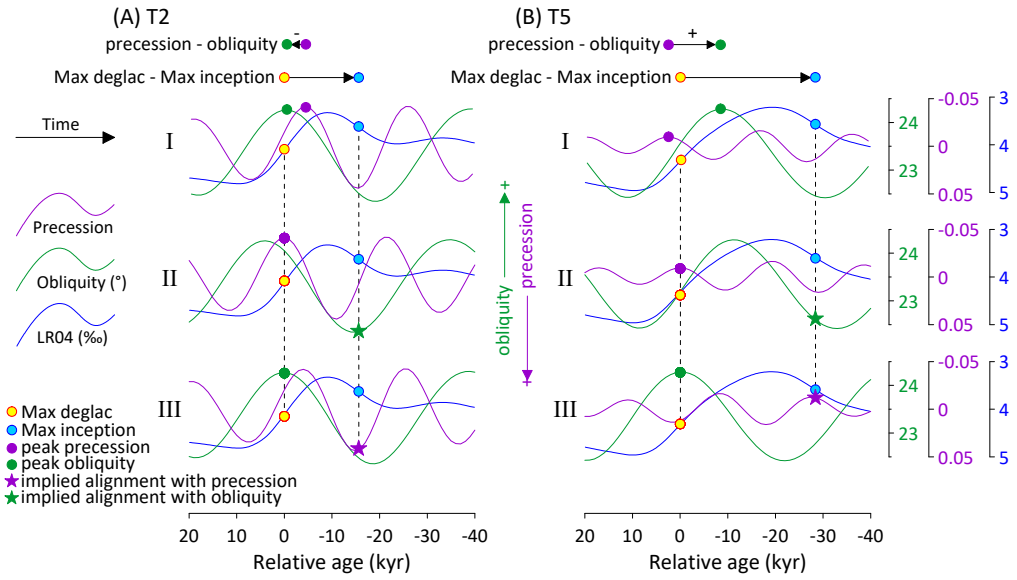

Fig. 3. Three scenarios for assessing which orbital parameter controls deglacial onset. Two deglacial intervals (A: T2 and B: T5) with contrasting orbital phasing illustrate the difference between Scenario I (original age models are accurate) versus Scenarios II and III, in which Max deglac is aligned with precession or obliquity respectively. Scenario II results in Max inception for both intervals being aligned consistently with respect to the phase of obliquity (which is expected when the correct starting parameter is chosen). In contrast, Scenario III results in misalignment of Max inception with respect to the phase of precession. See also Figure 4.

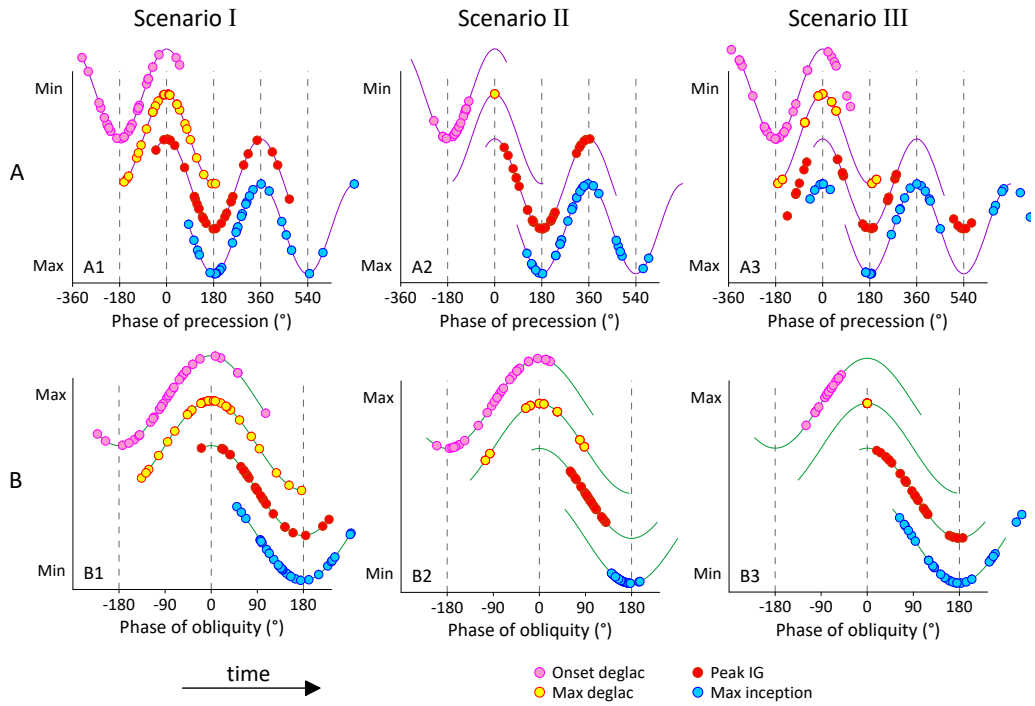

Fig. 4. Glacial inception aligns with obliquity when Max deglac is set to precession. Results for LR04_untuned, HW04 and U1476pmag from Scenarios I-III in Section 4. Each panel shows timing of Onset deglac, Max deglac, Peak IG and Max inception with respect to the phase of precession (row A) and obliquity (row B) for Terminations T2 to T12. In each case, zero phase is the closest precession/obliquity peak to Max deglac. Each individual point represents an individual termination/interglacial on one of the 3 timescales used. 10 terminations and 3 records gives a total of 30 points in each case (note some points are overlapping). Note in Scenario II (Max deglac set to peak precession; Part A2) much tighter clustering of Peak IG and Max inception with respect to obliquity (B2) as compared with Scenario I (B1). On the contrary, setting Max deglac to peak obliquity (Scenario III; B3) does not result in close alignment of Peak IG or Max inception with precession (A3). In addition, alignment between Onset deglac and Max deglac with respect to precession in Scenario III (A3) is significantly worse than in Scenario I (A1). See Figure S6 and Table S2 for more detail.

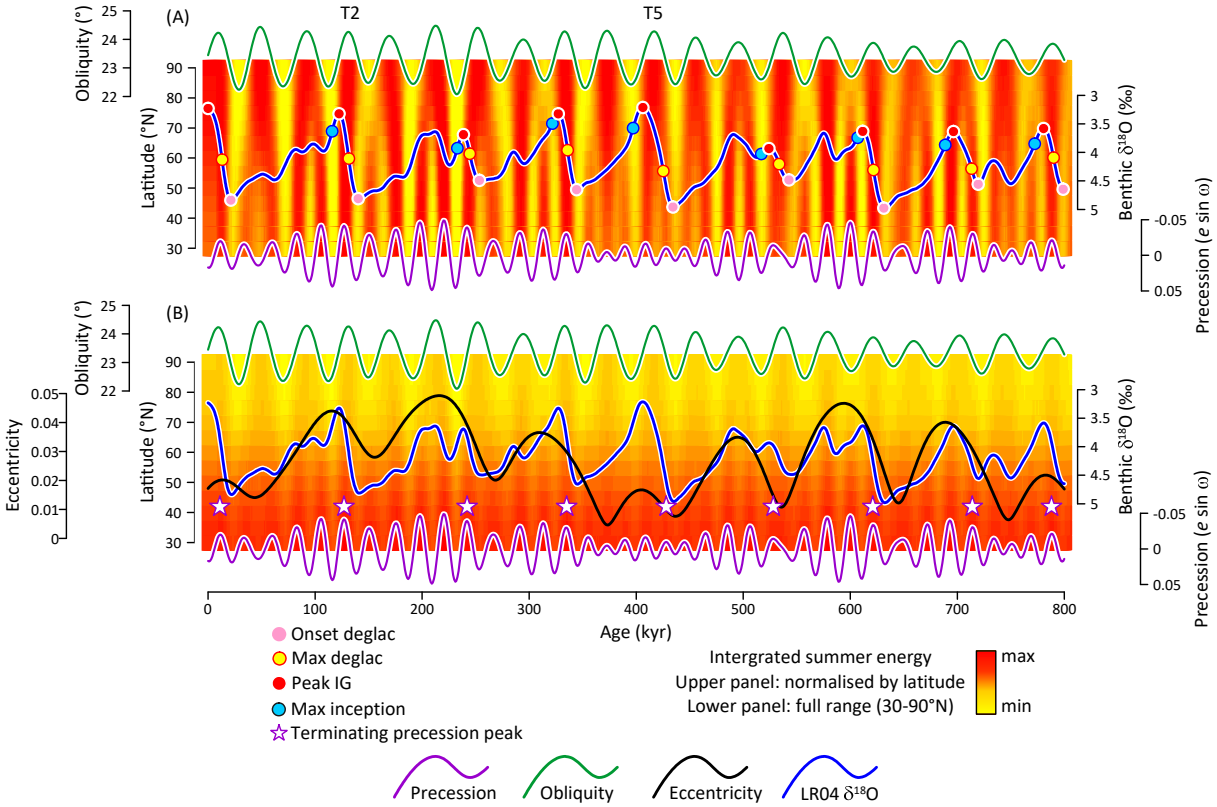

Fig. 5. Importance of latitude and inadequacy of a single insolation metric. (A) Upper and lowermost curves are obliquity and precession respectively (*72*), middle blue curve is the smoothed LR04 stack (*19*). Key events are indicated. Orange/yellow colors represent the integrated summer energy (*73*) normalized by each 5 degree band of latitude. Variability at lower latitudes is dominated by precession while higher latitudes (north of around 70°N) are dominated by obliquity. If deglaciation reflects the northward migration of the mean latitude (locus) of northern hemisphere land-based ice sheets, it can be appreciated why precession (at low latitudes) is more important for the earlier stages of deglaciation, while obliquity (at high latitudes) is more important for the end. No single insolation metric can be used to characterize this changing dependence. Note that for T5 (~420ka) precession and obliquity were out of phase, giving rise to a particularly long deglacial period as the initial stages of deglaciation gave way to the subsequent (lagged) development of full interglacial conditions. In contrast precession and obliquity were in phase during T2 (~130ka), resulting in a much shorter interval of deglaciation. (B) Same as (A) except that integrated summer energy is normalized across its entire range from 30 to 90°N. Ice sheets grow while eccentricity (black curve) decreases and obliquity is low. Purple stars are terminating precession peaks. Deglaciation may be triggered even if the amplitude of precession (a function of orbital eccentricity) is low (e.g. during T5) if ice sheets extend further to the south, where insolation is generally much higher than across more northerly latitudes.

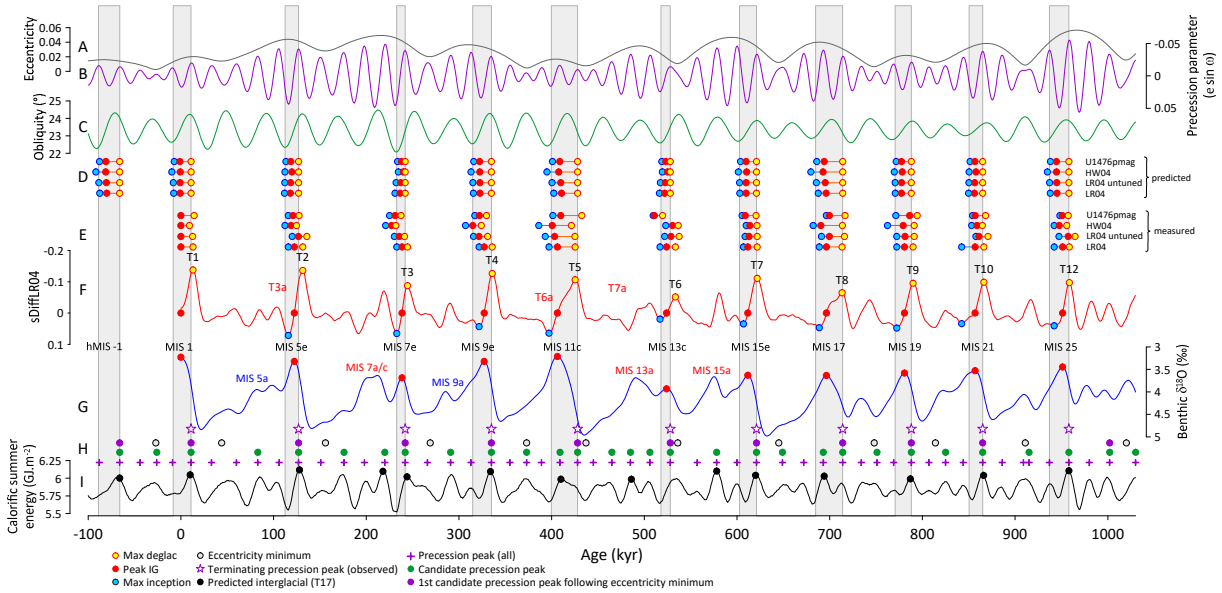

Fig. 6. Predicted occurrence and duration of glacial terminations and interglacials. (A-C) precession, obliquity and eccentricity (*72, 73*). (D) key events (Max deglac, Peak IG and Max inception) predicted from the relationships shown in Figs. 2C,D, S3,4. (E) same events measured directly from records of $\delta^{18}O$. (F) first differential of the LR04 stack (G). (H) Terminating precession peaks of the last 900kyr (purple stars and solid purple circles) are the subset of candidate peaks (green circles), which directly follow minima in eccentricity (grey circles). Candidate peaks are the subset of precession peaks (purple crosses) which begin when obliquity is increasing (or starts to increase within 2kyr of the turning point in precession (*16*)). (I) Integrated summer energy at 65°N (*73*) with black symbols indicating the predicted occurrence of interglacials based on the rule of ref (*10*) (T17). hMIS-1 is a hypothetical future interglacial. Vertical grey boxes indicate the predicted duration of interglacial periods (from Max deglac to Max inception) based on the average of predicted events in part (D).

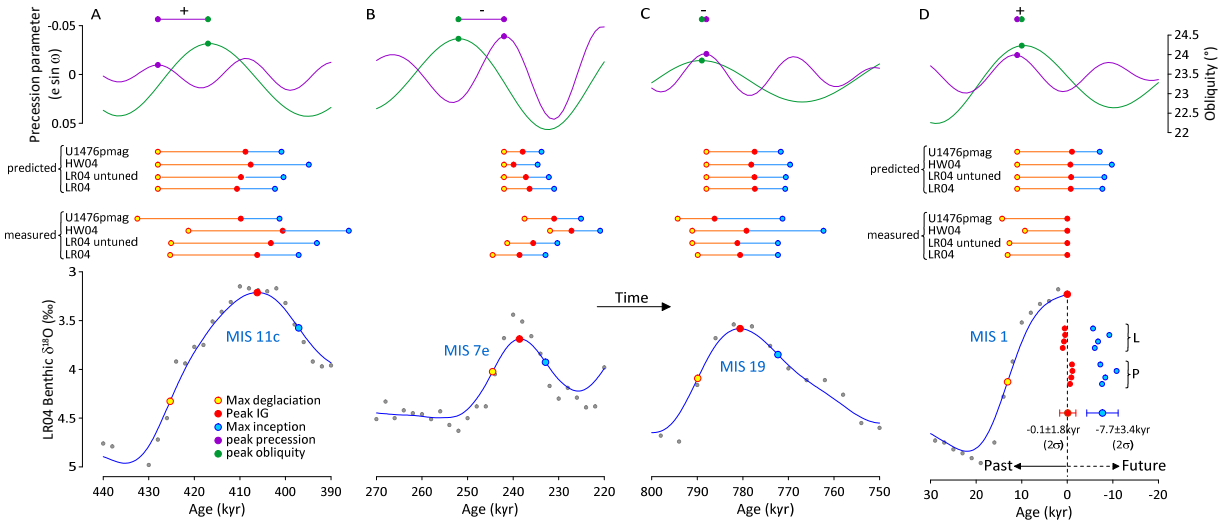

Fig. 7. Past and future predictions for the timing of Peak IG and glacial inception Note that time goes from left to right (A) Measured versus predicted occurrence of Max deglac, Peak IG and Max inception across T5 and MIS 11 (B, C) Same as (A) but for T3 (MIS 7e) and T9 (MIS 19) respectively. (D) Insolation variability across MIS 1 is similar to MIS 19. Isolated red and blue symbols are predictions of MIS 1 Peak IG and the next Max inception relative to Max deglac on LR04 (set L) and peak precession (set P) – see text.